Nanomed. J. 10(1): 59-67, Winter 2023

RESEARCH PAPER

Cytotoxicity and rapid uptake of antioxidants loaded onto solid lipid nanocarriers in MCF-7 and SK-Br-3 breast cancer cells

Faranak Aghaz [1], Soraya Sajadimajd [2], Saba Jalillian [1], Hessam Vaisiraygani [3], Mozafar Khazaei [4], Assad-vaisi Raygani [5, 4]*

[1]*Nano Drug Delivery Research Center, Faculty of Pharmacy, Health Technology Institute, Kermanshah University of Medical Sciences, Kermanshah, Iran*
[2]*Department of Biology, Faculty of Science, Razi University, Kermanshah, Iran*
[3]*Universita Gegli Studi Di Parma, Facolta Di Farmacia, Italia*
[4]*Fertility and Infertility Research Center, Health Technology Institute, Kermanshah University of Medical Sciences, Kermanshah, Iran*
[5]*Department of Clinical Biochemistry, Medical School, Kermanshah University of Medical Sciences, Kermanshah, Iran*

ABSTRACT

Objective(s): To eliminate the side effects of anti-cancer medications, the master plan is to use the nano-drug delivery system to deliver two or more anti-cancer medicines. This study aimed to use a binary drug delivery system to deliver Resveratrol (RES) and Tretinoin (TTN) to breast cancer cells and assess the effectiveness of this approach on two types of breast cancer cells (MCF-7 and SK-Br-3).

Materials and Methods: Binary-drug Solid Lipid Nanocarrier (SLN) formation was confirmed through dynamic light scattering (DLS), Fourier-transform infrared spectroscopy (FTIR), UV-vis spectrophotometers, and scanning electron microscopy (SEM). In this study, both breast cancer cell lines were cultured under various concentrations of free and dual drug (RES+TTN)-SLN.

Results: *In vitro* anticancer analysis, including MTT and quantitative reverse transcription-PCR (qRT-PCR) assays, revealed lower cell viability rates in both breast cancer cell lines compared with the control. Additionally, antiapoptotic-related genes were up-regulated and apoptotic-related genes were down-regulated when MCF-7 and SK-Br-3 were treated with RES+TTN-SLN. Furthermore, dual-encapsulation of RES and TTN significantly reduced cell viability percentage, even at the lowest concentrations (1 and 5 uM) compared with free drug and control groups for 48 hr. To sum it up, dual delivery systems of RES and TTN by SLN can deliver the optimal dose of RES and TTN into both MCF-7 and SK-Br-3 cell lines.

Conclusion: Conclusively, RES+TTN-SLN even at the lowest concentration (1 μM and 5 μM) showed a synergistic anti-cancer effect in MCF-7 and SK-Br-3 with a better enhancement of apoptotic gene expression by enhanced/controlled intracellular penetration.

Keywords: *Anti-oxidative effect, Apoptosis and anti-oxidant related genes, Breast cancer, Dual-drug delivery, MCF-7 and SK-Br-3, Synergistic anti-oxidative effect*

How to cite this article
Aghaz F, Sajadimajd S, Jalillian S, Vaisiraygani H, Khazaei M, Raygani AV. Cytotoxicity and rapid uptake of antioxidants loaded onto solid lipid nanocarriers in MCF-7 and SK-Br-3 breast cancer cells. Nanomed J. 2023; 10(1):59-67. DOI: 10.22038/NMJ.2022.66771.1704

INTRODUCTION

Although significant advances have been made in understanding and treating breast cancer today, it remains one of the deadliest causes of death worldwide, accounting for approximately 2.26 million deaths by 2030 [1, 2]. Currently, many researchers are looking for ways to reduce toxicity and increase the effectiveness of anti-cancer drugs [3].

Due to the void of toxicity in normal cells (non-cancerous), the effect of various anti-oxidants as anticancer drugs has been considered in the past decade. Resveratrol (3, 5, 4'-trihydroxystilbene) is an anti-inflammatory anti-oxidant, naturally produced in plants in response to injury or pathogen invasion. TTN, also known as all-trans

* *Corresponding author: Email: avaisiraygani@gmail.com*
Note. This manuscript was submitted on July 12, 2022; approved on Novamber 20, 2022

retinoic acid (ATRA), is an anticancer-anti-oxidant medicine. Given that multi-oxidative therapy approaches have been used in the past [4], the first evaluation of the synergistic effects of RES and TTN combinations on SK-Br-3 and MCF-7 cells was prompted by this finding. But, they have some limitations such as poor hydro-solubility, low biodisponibility, fast absorption and metabolism as well as tiny bio-life [5]. These characteristics likely limit the usefulness of exogenously applied RES and TTN as anti-oxidant and anti-apoptotic agents. By augmenting anti-oxidant stability and apparent solubility in water, nanoencapsulation may solve the above-detailed limitations and preserve anti-oxidant supplements' properties *in vitro*. Thus, the usage of nanotechnology for a more effective optimal transfer in anti-cancer drugs has been of much interest. The use of different nano forms of anti-oxidants such as TTN and RES was considered by researchers. One of the safest nano-methods for anti-cancer drug delivery is the solid lipid-nanoencapsulation (SLN) technique [6, 7]. In addition to protecting active ingredients from degradation, this method can also be used to label active ingredients with fluorescent probes, therefore making clinical evaluation much easier for researchers. So, it enhances the stability of anti-oxidant supplements and their solubility in water.

While nanomedicines have been extensively used in cancer treatment due to their ability to target cancer microenvironments effectively or latently without damaging normal tissues and defeat multidrug resistance, the heterogeneity of cancer cells, inefficiency of cellular uptake, and attenuation of anti-cancer effects have a significant impact on dissemination, inadequate stability *in vivo*, and attenuation of anti-cancer effects [8]. A total of two breast cancer cell lines were used for this experiment. Developed from pleural effusion, MCF-7 is a noninvasive cell line obtained from a female with low metastatic potential. SK-Br-3 is a cell line gathered from a pleural effusion. This cell line is capable of creating inadequate differentiated tumors.

To the best of our knowledge, the preparation of lipid-core nano encapsulated RES and TTN (RES+TTN-SLN) has not been reported yet. Therefore, through modulation of the breast cancer progression, we evaluated the anticancer activity of RES+TTN-SLN to combat the proliferation of HER2-positive and HER2-negative breast cancer models. In addition, for the quantification study and comparison, internalization, and uptake mechanism of RES+TTN-SLN, as novel anti-cancer therapies, MCF-7 and SK-Br-3 were used together.

MATERIALS AND METHODS

Materials

Sigma-Aldrich (St. Louis, MO, USA) donated the following supplies: Stearic acid, Sodium tripolyphosphate solution (TPP), Polysorbate 80 (Tween 80), Dimethyl sulfoxide (DMSO), CH_2CL_2, Tretinoin (TTN) and trans-Resveratrol - 3,4' - (CAS Number: 501-36-0 99 percentage, HPLC) (RES). All other chemicals and solvents were provided by Merck (Germany), including ethanol, acetone, buffer ingredients, and ultrapure water was attained from Milli-Q (Millipore, Bedford, MA, USA).

Preparation of RES+TTN-SLN

To obtain the TTN+RES-SLN formulations with a particle size of 200 nm or smaller, the modified previous self-assembly method was used in this study [9]. Briefly, RES and TTN were solved (CH_2Cl_2 and DMSO, respectively) and added to one milliliter of lipid at room temperature (25 °C), which was then sonicated for 120 sec at 80 WT, then freeze-dried and stored at -20 °C. Also, the blank-SLN (B-SLN) was synthesized with a similar method. We examined the physical aesthetics, convenience of re-constitution, and quality characteristics of the nanocapsules when added to cell culture media.

Determination of EE and DL %

Following the centrifugation at 18,200×g for ten minutes at room temperature to produce the pellet (loaded drug) and supernatant (un-entrapped drug), the supernatant of the stock formulations was analyzed with a UV-VIS spectrophotometer, at wavelengths 297 and 360 nm for RES and TTN and determination of entrapment efficiency (EE%) and drug loading (DL%) [10]. Calibration curves were created with a straight line and R2 of 0.9988 for RES and 0.9868 for TTN. The DL% and EE% of RES, TTN, or RES+TTN-SLN were calculated by the formula given below:

EE%: [Total drug −Free drug / Total drug] ×100.

DL%: [Total drug −Free drug / total weight nanoparticles] ×100.

All measurements were done in triplicate, and the data were presented as mean ± S.D.

In vitro drug release

We assessed TTN and RES released from RES+TTN-SLN using a dialysis bag method (Sigma Aldrich, molecular weight cut off-20 kD) [11], in phosphate buffer (pH = 7.4). Briefly, 4 ml of the RES+TTN were placed in a dialysis bag which was immersed in 80 ml of phosphate buffer solution (pH = 7.4) and put in a shaker incubator (200 rpm at 37 °C, for 55 hr. During different intervals of time (0, 1, 2, 3, 4, 5, 6, 24, 48, and 55 hr), 1 ml of the release medium was removed and replaced with fresh PBS of the same volume. Then TTN and RES were quantified by a UV-vis spectrophotometer set (Philips PU 8620, U 360 nm for TTN) at two different absorption maxima (λ max), corresponding to 297 nm for RES and 360 nm for TTN. Drug quantification for the *in vitro* drug release profile was calculated as a percentage of the drug release quantity at each time interval relating to the amount of drug trapped within the SLN. The experiment was repeated identically in triplicate

Fourier transform infrared spectroscopy (FT-IR)

By the potassium bromide disk method, FT-IR spectroscopy of synthesized compounds was used to assess the chemical interaction of different functional groups. 1–2 mg of the samples was mixed and triturated with potassium bromide (100 mg). An FT-IR spectrophotometer set (IR prestige-21, Shimadzu Co., Japan) was used to measure the spectra of free anti-oxidants (RES/TTN), B-SLN, and RES+TTN-SLN over 200–40000 cm^{-1} with a resolution of 4 cm^{-1} to determine any shift in individual peaks of the drugs.

Storage stability

A freeze-dried RES+TTN-SLN nanoencapsule was stored at -20 °C in sealed vials. Following the assessment of physical appearance and ease of reconstitution, the freeze-dried nanoencapsules were tested for storage stability after two months.

In vitro biological evaluation of RES+TTN-loaded SLN

Cell culture model

In the present study, the MCF-7 and SK-Br-3 cell cell line (Pasteur Institute of Iran) was used as an *in vitro* model. These cells were cultured in RPMI1640 supplemented with 10 percent fetal bovine serum (FBS) and 100 U/ml penicillin and preserved at 5 percent CO2, 37 °C, and humidified air atmosphere during the research. An average medium renewal was made every day and viable cells were counted using a hemocytometer, based on their abilities to exclude trypan blue. Drug treatment was usually performed 24 hr after seeding the cells.

Cell viability assay

MTT assays were used to evaluate the drug's cytotoxicity on both cell line types (Density; 5 × 103 cells/cm2). Briefly, MCF-7, and SK-Br-3 cells were seeded in 96-well culture and treated with Blank-SLN and RES+TTN-SLN for 24 and 48 hr, at PH 7.4. The media were replaced with 50 µl of MTT solution (5 mg/ml). After 4 hr incubation, 150 µl of DMSO was added to dissolve the formazan crystals. Then, the absorbance of each well was read at 570 nm using the ELISA reader (Exert 96, Asys Hitch, Ec Austria). The formula below was used to calculate the cell viability percentage:

$$\text{Cell viability (\%)} = \frac{A570\,(sample)}{A570(control)} \times 100$$

Based on triplicate independent experiments conducted, the values were expressed as mean±SD.

Gene expression analysis

Quantitative real-time PCR

To obtain cDNA from the supplement, the TRIzol method (Invitrogen, Carlsbad, USA) was used to extract total RNA from cells. After quantification, RNA was reverse-transcribed with Applied Biosystems cDNA Reverse Transcription Kit (Applied Biosystems, Carlsbad, USA). Apoptosis-related genes, including BCL-2-associated X protein (Bax) and BCL-2 apoptosis regulator (BCL-2), were assessed with Syber green quantitative real-time polymerase chain reaction (RT-PCR, ABI ViiA 7; Applied Biosystems, Foster City, CA, USA). The following primers were used: Bax, 5'- CGAGCTGATCAGAACCATCA-3' (forward) and 5'-GAAAAATGCCTTTCCCCTTC-3' (reverse); BCL-2, 5'- TACCGTCGTGACTTCGCAGAG-3' (forward) and 5'- GGCAGGCTGAGCAGGGTCTT-3' (reverse). qRT-PCR was performed with a 5-min initial denaturation at 95 °C followed by 40 three-step cycles of 30 sec at 95 °C (denaturation), 30 sec at 55 °C (annealing), and 30 sec at 72 °C (extension). All primers were ordered from Microsynth (Qiagen, Valencia, CA, USA) [12, 13].

After qRT-PCRs, data were analyzed using the 2 -ΔΔCT method, as previously defined [14], and

each experiment had a complete replicate of the reactions. The standard curves were prepared with progressive cDNA dilutions of the qRT-PCR Master Mix (Fermentas GmbH, St. Leon-Rot, Germany).

Statistical analysis

The data attained from the different assays were statistically analyzed using SPSS (version 23.0), one-way ANOVA, and control samples were considered as 100 percent viability for each time point. All the experiments were performed with three biological replicates and each data is presented as mean ± standard deviation (SD). A *P*-value of≤ 0.05 was considered to show a statistically significant difference. Cell cultures of SK-Br-3 and MCF-7 without were used as experimental controls.

Data availability

Detailed data supporting the study's findings can be found in this paper. On reasonable request from the corresponding authors, the raw and analyzed datasets created through the present study are accessible for research purposes.

RESULTS

Preparation and physicochemical properties of TTN+RES-SLN

The dialysis process was used to prepare RES+TTN-SLN [15]. We describe the physicochemical properties of RES+TTN-SLN with 183 nm in size (Fig. 1). In this formulation, there was a PDI of 0.17 demonstrating no agglomeration and an exceptional dispersion of the particles (Fig. 1). The morphological studies of RES+TTN-SLN by SEM show that the particles are spherical (Fig. 2). The UV-Vis spectrophotometry results showed that amounts of DL in RES+TTN-SLN formulation were 21% and 98 % for TTN, and 24 % and 87 % for RES. Based on these results, RES+TTN-SLN reasonably exhibits a spherical shape, regular distribution, size uniformity (183 nm), and good monodispersity.

FT-IR analysis

As seen in Fig. 3, free anti-oxidants (TTN and RES), B-SLN, and RES+TTN-SLN complexes were

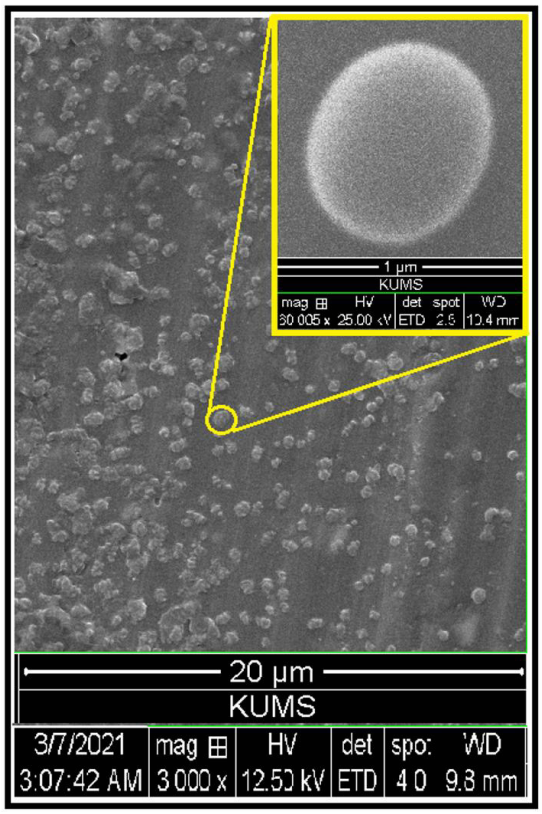

Fig. 2. SEM image: morphology analysis of TTN+RES-SLN

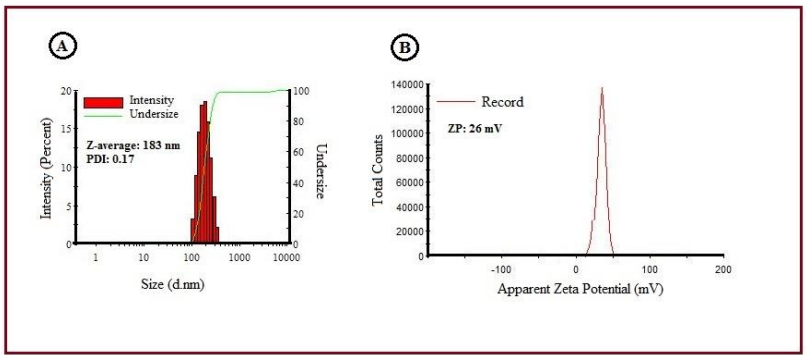

Fig. 1. Physicochemical characterization of TTN+RES-SLN by the Zetasizer instrument; (A) particle size distribution and (B) Zeta potential

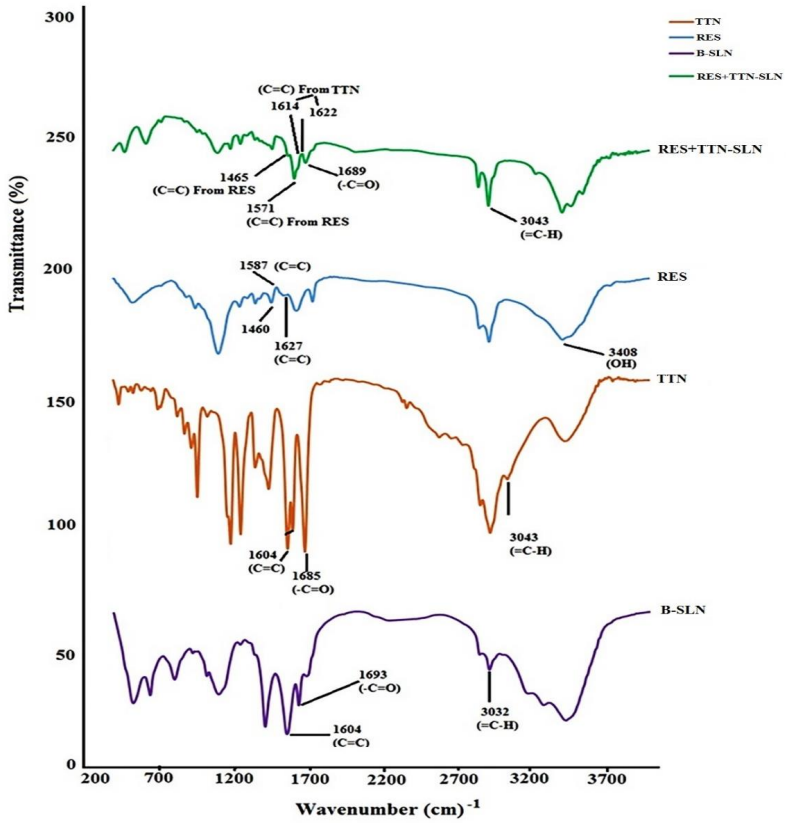

Fig. 3. FT-IR diagrams of the SLNs: B-SLN (a), TTN (b), RES (c), and TTN+RES-SLN (d)

all FTIR spectra. In the B-SLN spectrum, the C=C stretching of SLN is identifiable at 1604 cm^{-1}; the O=C stretching is seen at 1693 cm^{-1}; the OH stretching of carboxylic acids in SLN is detected at 2500–3600 cm^{-1}, and the double bands appear at 3032 cm^{-1}. At 3600–2500 cm^{-1} (OH stretching), 2500–3600 cm^{-1} (OH stretching of carboxylic acid from TTN and SLN), 1690 and 3043 cm^{-1} (C=O and =C-H groups of TTN and SLN), and 3415 and 1606 cm^{-1} (N-H stretching and bending vibration of SLN); a weak peak of double bands =C-H stretch appeared at 3043 cm^{-1} in TTN spectrum.

The spectrum of RES shows peaks at 3415 and 1620 cm^{-1} (N-H stretching, respectively), 1610, 1570, 1465 cm^{-1} (C=C stretching, respectively), 1691 cm^{-1} (-C=O stretching, R–COOH carbonyl stretching), 2500–3600 cm^{-1} (OH stretching, carboxylic acid from SLN), and a weak peak at 3035 cm^{-1} (=C–H stretching).

The complex of TTN, RES, and SLN peaks was observed in the spectrum of RES+TTN+SLN (Fig. 3). During its spectrum analysis, sharp peaks were observed at 1689 cm^{-1} (C=O stretching from SLN R–COOH carbonyl), 2500–3600 cm^{-1} (OH stretching from TTN), 1571 and 1465 cm^{-1} (C=C stretching from RES), 1622 and 1614 cm^{-1} (C=C stretching from TTN and RES) and weak peaks of 3043 cm^{-1} (=C–H stretch) or 2850–2927 cm^{-1} (CH_2 and CH_3 stretching from TTN and RES). The comparison of the RES+TTN-SLN spectrum (Fig. 3) to free anti-oxidants (RES/TTN) reveals a significant shift in the position of the peaks at 3439, 1693, 1629, 1639, and 1570 cm^{-1} in free RES/TTN-SLN to 3415, 1689, 1614, 1606, and 1571 cm^{-1} in RES+TTN-SLN complex, demonstrating the presence of TTN, RES, and SLN molecules absent any chemical interaction between them.

In vitro drug release

We performed *in vitro* study of the RES+TTN-SLN release profile, during 72 hr (Fig. 4) our results showed a controlled release of both anti-oxidants from RES+TTN-SLN, without an apparent burst of release (lower than 35% for both RES and TTN). In contrast, TTN and RES were released from the free anti-oxidant at a faster rate: 50% within 10 hr, 90% within 24 hr, and finally 100% within 28 hr of incubation.

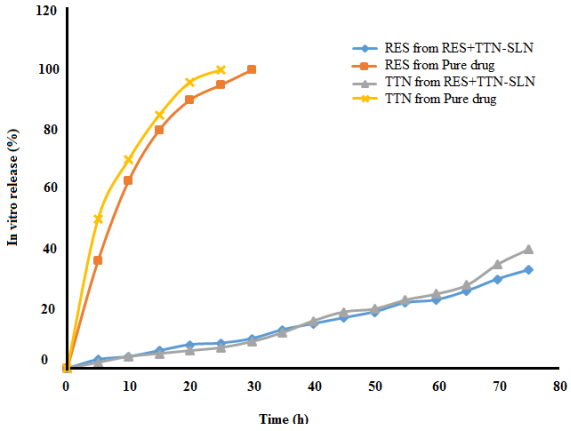

Fig. 4. *In vitro* drug release profiles of TTN and RES from TTN+RES-SLN

In vitro efficacy evaluation

Anti-cancer effects of RES+TTN-SLN on MCF-7 and SK-Br-3 cell line

Experiment 1: In this experiment, the effects of various concentrations of 0, 1, 5, 10, 20, 40, 80, and 100 µM of RES+TTN-SLN and B-SLN on the cell viability percentage of MCF-7 cell line during 24 and 48 hr were examined. The viability percentage of MCF-7 cells decreased when both drugs were co-encapsulated with RES/TTN at all doses examined. In comparison with co-encapsulation RES/TTN, free RES or TTN drugs did not cause such a steep decline in the viability percentage of MCF-7 cells. These results suggest that the anti-oxidants examined in this RES+TTN-SLN confer a synergistic effect. Increasing the dosage of co-encapsulation RES/TTN from 1 to 5 µM resulted in about a 15 percent decrease in cell viability from 60 percent to 45 percent. After increasing the dosage from 5 to 20 µM, cell viability percentage continued to decrease, which remained unchanged for dosages of 40, 80, and 100 µM (Fig. 5).

Experiment 2: In this study, several concentrations of 0, 1, 5, 10, 20, 40, 80, and 100 µM of RES+TTN-SLN and B-SLN on SK-Br-3 cell viability percentage were examined. For the analysis of the SK-Br-3 cell line, the dosage of 40 µM on viability has been effective, and the most mortality was observed in dosages of 80 µM and 100 µM. A considerable decrease in cell viability percentage is observed within 40 µM dosages of co-encapsulation RES+TTN-SLN since there is more than 40 percent molarity in 80 and 100 µM. In the MCF-7 cell line, however, this considerable decrease was observed at 1 µM dosage of co-encapsulation RES+TTN-SLN (Fig. 5).

Evaluation of RES+TTN-SLN treatments on the apoptosis-expression-related genes

In the analysis of the BCL-2 and Bax genes, different concentrations of B-SLN did not show a significant effect compared with the control group. Based on our result, BCL-2 gene expression decreased significantly in the MCF-7 cell line, whereas this gene expression did not decrease significantly on SK-Br-3 in the free RES+TTN group compared with the control. In the RES+TTN-SLN group BAX gene expression was significantly increased just in the MCF-7 cell line, not in SK-Br-3. Also, BCL-2 gene expression was significantly reduced in both cell lines (MCF-7 and SK-Br-3) (Fig. 6) in this group compared with the control. It is evident from these results that the studied anti-oxidants have synergized effect in co-

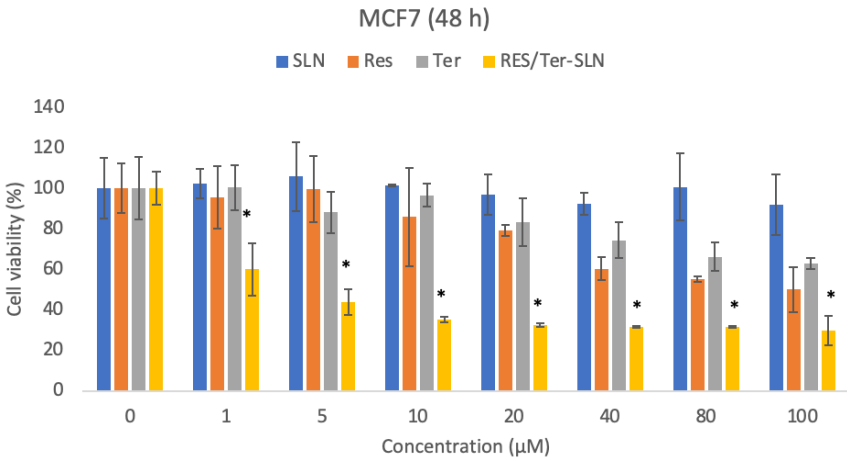

Fig. 5. MTT assay of MCF-7 cell line after 48 hr.

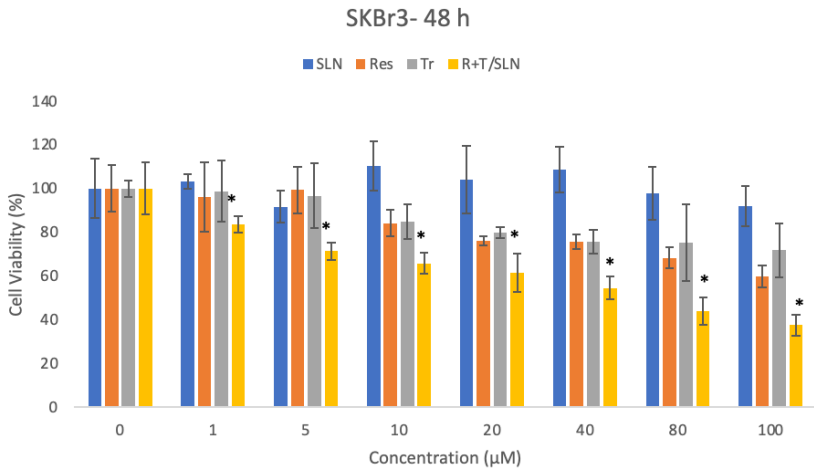

Fig. 6. MTT assay of SK-Br-3 cell line after 48 hr.

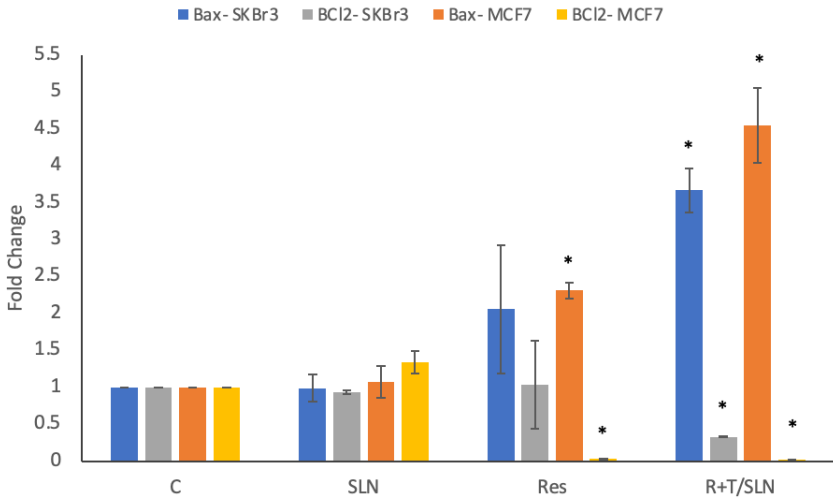

Fig. 7. BAX and BCL-2 gene expression in treated MCF-7 and SK-Br-3 cell lines

encapsulation form.

DISCUSSION

Tumor breast cells show higher ROS levels to maintain low levels of oxidative stress compared with their normal cells [16]. It makes sense to use exogenous anti-oxidants or their combination to treat breast cancer [17]. However, poor water solubility, low responsibility, and their short bioavailability have led to problems in *in vitro* and *in vivo* evaluations. The function of the nano drug delivery system is to overcome the weakness of varied chemotherapy drugs [18, 19] due to its favorable structure for improvement in drug stability, without passenger biotoxicity [20]. SLNs are formed of a hard lipid matrix and a surfactant layer, and because of their properties, they can load enough water-soluble drugs, delivering them at defined rates and accordingly enhancing their intracellular uptake. These properties urged us to use SLNs as carriers for optimal dose delivery of RES and TTN and evaluate their synergistic anticancer effects on SK-Br-3 and MCF-7 cell lines. Considering our previous studies regarding suitable formulations and the best solvent structure and lipid nucleus (reference), SLNs were used for this study.

Synthesis and physicochemical characterization of RES/TTN-SLN was confirmed by FTIR, UV-vis spectrophotometer, SEM, and zeta sizer analysis. According to our results, this synthetic system could facilitate the passage of drugs across

biological barriers and provide better integration for the delivery of RES/TTN into the subcellular compartments of the cell, such as mitochondria and nuclei [21]. In normal physiological PH (7.4), the TTN+RES-SLN surface charge is greater than -17 mV suggesting higher physical stability and preventing particles from aggregating. Additionally, synthesized TTN+RES-SLN has a slightly narrow size distribution (PDI =0.17) and a high encapsulation efficiency (EE %> 98 %). It is evident from the small values of PDI that the NPs are homogeneous in size. Also, the mean particle diameter was 183 nm and this small size caused the higher cellular uptake. Moreover, SEM observations showed that TTN+RES-SLN illustrated a spherical shape and good distribution, which indicates superior capping intensity. Therefore, all of these nanoencapsules' basic-physicochemical properties are most likely reasons for the higher cellular uptake of TTN+RES-SLN in both cell lines.

Our cytotoxicity results from produced TTN+RES-SLN indicated an anticancer effect as well as decreased cell viability percentage on both cell lines. In accordance with our research team, Abdel-Hakeem *et al*. indicated decreased MCF-7 cell viability percentage due to the use of anti-oxidants [24].

Our results from both experiments indicate that RES+TTN-SLN at the lowest concentration (0.1 µM +0.25 µM) was able to decrease the expression of the BAX gene. It was also seen in our results that the gene expression of BCL-2 was increased compared with the control group. Increased BCL-2 gene expression observed in both MCF-7 and SK-Br-3 treated by RES+TTN-SLN is commonly attributed to in-synergist dose-optimal bioavailability of RES and TTN. By achieving this result, the drug is released for a longer period of time, and with a lower dose than they when freely administered. Similar to the present study, a study published by Gupta *et al*. demonstrated the beneficial anti-oxidant and anticancer activity of diosgenin-enriched Paris polyphyletic rhizome extract (DPPE) anti-oxidant from MCF-7 cell lines. They also demonstrated that DPPE-anti-oxidant suppressed BCL-2 and raised Bax expression in the MCF-7 cell line, in line with ours [25].

CONCLUSION

This study aimed to investigate the synergistic anti-oxidant and anticancer efficacy of RES and TTN in each breast cancer cell line (MCF-7 and SK-Br-3). At 1 and 5 M concentrations, we found that RES-TTN-SLN has synergistic anti-cancer activities by inhibiting cell proliferation through improving RES and TTN penetration into cells. This is due to the lower particle size ≤200 nm, PDI of 0.17, high zeta potential, their high EE % or DL %, monodisperse form, and slow/simultaneous release of RES and TTN from RES+TTN-SLN, as opposed to free RES/TTN. Also, we found that co-encapsulations released fewer doses of RES and TTN, which led to higher gene expression of apoptosis in both cancer cells, even at the lowest concentrations (5 and 10 µM). Collectively, the current research demonstrated greater practical efficacy for dual-delivery-SLN than free antioxidants at a point in time for each of the MCf-7 and SK-Br-3.

ACKNOWLEDGMENTS

Not Applicable.

FUNDING

This study was funded by the National Institute for Medical Research Development (NIMAD, 987697).

CONFLICTS OF INTEREST

The authors declared that they have no competing interests.

REFERENCE

1. He B, Sui X, Yu B, Wang S, Shen Y, Cong H. Recent advances in drug delivery systems for enhancing drug penetration into tumors. Drug Deliv. 2020;27(1):1474-90.
2. Ryser MD, Lange J, Inoue LY, O'Meara ES, Gard C, Miglioretti DL, et al. Estimation of breast cancer overdiagnosis in a US breast screening cohort. Ann. Intern. Med. 2022; 175(4):471-478
3. Gunasekaran G, Bekki Y, Lourdusamy V, Schwartz M. Surgical treatments of hepatobiliary cancers. J. Hepatol. 2021;73:128-36.
4. Ellis C, Millikan L, Smith E, Chalker D, Swinyer L, Katz I, et al. Comparison of adapalene 0· 1% solution and tretinoin 0· 025% gel in the topical treatment of acne vulgaris. Br. J. Dermatol. 1998;139(52):41-47
5. Dehaghani MZ, Yousefi F, Seidi F, Bagheri B, Mashhadzadeh AH, Naderi G, et al. Encapsulation of an anticancer drug Isatin inside a host nano-vehicle SWCNT: a molecular dynamics simulation. Sci. Rep. 2021;11(1):1-10.
6. Amer Ridha A, Kashanian S, Rafipour R, Hemati Azandaryani A, Zhaleh H, Mahdavian E. A promising dual-drug targeted delivery system in cancer therapy: nanocomplexes of folate–apoferritin-conjugated cationic solid lipid nanoparticles. Pharm Dev Technol. 2021;26(6):673-81.
7. Zhang Y, Uthaman S, Song W, Eom KH, Jeon SH, Huh KM, et al. Multistimuli-responsive polymeric vesicles

for accelerated drug release in chemo-photothermal therapy. ACS Biomater. Sci. Eng. 2020;6(9):5012-23.
8. Aghaz F, Vaisi-Raygani A, Khazaei M, Arkan E, Sajadimajd S, Mozafari H, et al. Co-encapsulation of tertinoin and resveratrol by solid lipid nanocarrier (SLN) improves mice in vitro matured oocyte/morula-compact stage embryo development. Theriogenology. 2021;171:1-13.
9. Motiei M, Kashanian S. Novel amphiphilic chitosan nanocarriers for sustained oral delivery of hydrophobic drugs. Eur. J. Pharm. Sci. 2017;99:285-91.
10. Herndl GJ, Kaltenböck E, Müller-Niklas G. Dialysis bag incubation as a nonradiolabeling technique to estimate bacterioplankton production in situ. Handbook of Methods in Aquatic Microbial Ecology: CRC Press; 2018; 4(1): 553-556.
11. Dhivya S, Gayatri Devi R, Selvaraj J, Jothi Priya A. Regulation of Chloride Intracellular Channel Protein 1 and Caspase-3 mRNA Expression by Hydroethanolic Extract of Aegle marmelos Fruit Human Breast Cancer Cell Line-MCF-7. J. Pharm. Res. Int. 2021;33(47):587-593
12. Biresaw SS, Taneja P. Copper nanoparticles green synthesis and characterization as anticancer potential in breast cancer cells (MCF7) derived from Prunus nepalensis phytochemicals. Materials Today: Proceedings. J. Pharm. Res. Int. 2022;49:3501-3509.
13. Livak KJ, Schmittgen TD. Analysis of relative gene expression data using real-time quantitative PCR and the 2− ΔΔCT method. methods. 2001;25(4):402-408.
14. Xiao H, Song H, Yang Q, Cai H, Qi R, Yan L, et al. A prodrug strategy to deliver cisplatin (IV) and paclitaxel in nanomicelles to improve efficacy and tolerance. Biomaterials. 2012;33(27):6507-19.
15. Totten SP, Im YK, Cepeda Cañedo E, Najyb O, Nguyen A, Hébert S, et al. STAT1 potentiates oxidative stress revealing a targetable vulnerability that increases phenformin efficacy in breast cancer. Nat. Commun. 2021;12(1):1-20.
16. Griñan-Lison C, Blaya-Cánovas JL, López-Tejada A, Ávalos-Moreno M, Navarro-Ocón A, Cara FE, et al. Antioxidants for the treatment of breast cancer: Are we there yet? Antioxidants. 2021;10(2):205.
17. Carbone C, Fuochi V, Zielińska A, Musumeci T, Souto E, Bonaccorso A, et al. Dual-drugs delivery in solid lipid nanoparticles for the treatment of Candida albicans mycosis. Colloids Surf. B. 2020;186:110705.
18. Huo M, Wang H, Zhang Y, Cai H, Zhang P, Li L, et al. Co-delivery of silybin and paclitaxel by dextran-based nanoparticles for effective anti-tumor treatment through chemotherapy sensitization and microenvironment modulation. JCR.2020;32(10):198-210
19. Campos J, Severino P, Santini A, Silva A, Shegokar R, Souto S, et al. Solid lipid nanoparticles (SLN): prediction of toxicity, metabolism, fate and physicochemical properties. Nanopharmaceuticals. 2020;10(1):1-15.
20. Gaber M, Elhasany KA, Sabra S, Helmy MW, Fang J-Y, Khattab SN, et al. Co-administration of tretinoin enhances the anti-cancer efficacy of etoposide via tumor-targeted green nano-micelles. Colloids Surf. B. 2020;192(1):110997.
21. Abdel-Hakeem MA, Mongy S, Hassan B, Tantawi OI, Badawy I. Curcumin Loaded Chitosan-Protamine Nanoparticles Revealed Antitumor Activity Via Suppression of NF-κB, Proinflammatory Cytokines and Bcl-2 Gene Expression in the Breast Cancer Cells. J. Pharm. Sci. 2021;110(9):3298-305.
22. Gupta DD, Mishra S, Verma SS, Shekher A, Rai V, Awasthee N, et al. Evaluation of antioxidant, anti-inflammatory and anticancer activities of diosgenin enriched Paris polyphylla rhizome extract of Indian Himalayan landraces. J. Ethnopharmacol. 2021;270:113842.